

Electronic Supplementary Information

What are the key factors governing the nucleation of CO₂ hydrate?

Zhongjin He, Praveen Linga and Jianwen Jiang*

Department of Chemical and Biomolecular Engineering, National University of Singapore, 117576, Singapore

Simulation Methods

In a previous study, we conducted microsecond molecular dynamics (MD) simulations on the nucleation and growth of CH₄/CO₂ mixed hydrates from two-phase systems of water and CH₄/CO₂ gas mixture.¹ At that time, we also performed simulations to explore the nucleation of CO₂ hydrate from water/CO₂ two-phase system at 250 K and 50 MPa using the TIP4P-Ice water model and the EPM2 CO₂ model; however, the nucleation was not observed even though the simulation duration was up to 7 μ s, as shown in Fig. S1. In the current study, we therefore attempt to unravel the key factors governing the nucleation of CO₂ hydrate.

In a cubic box with an initial length of 5 nm, 512 CO₂ molecules and 2944 water molecules were randomly mixed to form a homogenous system. The composition of the system was the same as a sI crystalline hydrate. The system was initially equilibrated under isothermal-isobaric (NPT) ensemble at 300 K and 10 MPa for 20 ns to spontaneously form a spherical CO₂ phase in water. Such a two-phase system (Fig. S2A), as the starting configuration, was cooled and pressurized to 250 K and 50 MPa, and simulated for up to several μ s to examine CO₂ hydrate nucleation. The TIP4P-Ice model² was used for water and the cross-interaction parameters between water and CO₂ were calculated by the Lorentz-Berthelot combining rules. As mentioned above, CO₂ hydrate nucleation did not occur using the EPM2 CO₂ model³ (Fig. S1A, S1C, S1E and S1F). Subsequently, the TraPPE CO₂ model⁴ was tested but nucleation did not occur either (Fig. S1B, S1D, S1E and S1G). Recently, Costandy *et al.*⁵ examined a series of water models and CO₂ models to simulate the phase equilibria of CO₂ hydrate; they found that the three-phase coexistence temperature of CO₂ hydrate and the solubility of CO₂ in water could be accurately predicted by using the TraPPE CO₂ model and the TIP4P-Ice model *with the well depth between the oxygen in CO₂ and the oxygen in water $\epsilon_{O(CO_2)-O(H_2O)}$ scaled by a factor of 1.08*. Thus, we used these optimized parameters to explore CO₂ hydrate nucleation and found that CO₂ hydrate nucleation occurred, with a pre-nucleation CO₂ mole fraction in water x_{CO_2} (about 0.080) higher than the cases using the EPM2 (about 0.068) and TraPPE (about 0.064) CO₂ models. These results unravel that a high aqueous guest concentration is required to trigger CO₂ hydrate nucleation. Repeat runs were performed (2 runs using the EPM2 or TraPPE CO₂ models and 5 runs using the optimized parameters). To further explore whether CO₂ hydrate nucleation can occur at a lower x_{CO_2} using the optimized parameters, we manually set up a water/slab CO₂ two-phase system as the starting configuration (Fig. S2B). This system also contained 512 CO₂ molecules and 2944 water molecules and its box size was 3.46 \times 3.46 \times 11.00 nm³. It showed a lower x_{CO_2} (about 0.060) than the water/spherical CO₂ two-phase system (about 0.080), due to the lower Young-Laplace pressure at the planar water/CO₂ interface. Additionally, the simulation results on CH₄ hydrate nucleation from our previous study¹ were used to compare the nucleation of CO₂ and CH₄ hydrates at the same condition (512 CH₄ and 2944 water molecules at 250 K and 50 MPa).

To confirm that a high aqueous guest concentration is required for CO₂ hydrate nucleation and quantitatively determine the critical CO₂ concentration for nucleation (especially in the simulations using the EPM2 or TraPPE CO₂ models, where nucleation did not occur), we set up a series of homogenous CO₂ solution systems as starting

configurations to examine CO₂ hydrate nucleation at 250 K and 50 MPa. 2944 water molecules and different number of CO₂ molecules (512, 479, 440, 401, 364, 327, 291, 256, 222, 188 and 155 CO₂) were randomly placed in a cubic box to form homogenous CO₂ solution systems with different x_{CO_2} . The EPM2, TraPPE CO₂ models and the optimized CO₂–water parameters were used and the simulation duration was at least 500 ns. Note that during the simulations, x_{CO_2} was lower than that in the starting configurations, as some CO₂ molecules aggregated to form small clusters. Particularly, a large CO₂ phase formed in the system with the highest CO₂ supersaturation (512 CO₂) using the EPM2 and TraPPE CO₂ models, see Fig. S1H and Fig. S9F. Table S1 summarizes the simulation systems in this study.

Table S1. Summary of the simulation systems in this study.^a

| System | Runs | CO ₂ model | Water model | Combining rule | x_{CO_2} | Nucleation state |
|---------------------------------|----------------|-----------------------|-------------|---|--|---|
| Water/Spherical CO ₂ | 2 | EMP2 | TIP4P-Ice | Lorentz-Berthelot | 0.068 | not nucleated |
| Water/Spherical CO ₂ | 2 ^b | TraPPE | TIP4P-Ice | Lorentz-Berthelot | 0.064 | not nucleated |
| Water/Spherical CO ₂ | 5 | TraPPE | TIP4P-Ice | 1.08* $\epsilon_{\text{O}(\text{CO}_2)\text{-O}(\text{H}_2\text{O})}$ | 0.080 | nucleated |
| Water/Slab CO ₂ | 2 | TraPPE | TIP4P-Ice | 1.08* $\epsilon_{\text{O}(\text{CO}_2)\text{-O}(\text{H}_2\text{O})}$ | 0.060 | not nucleated |
| CO ₂ solutions | 1 | EMP2 | TIP4P-Ice | Lorentz-Berthelot | No. of CO ₂ 188-512 | nucleated at $x_{\text{CO}_2} \geq 0.088$ |
| CO ₂ solutions | 1 | TraPPE | TIP4P-Ice | Lorentz-Berthelot | No. of CO ₂ 188-512 ^b | attempts at $x_{\text{CO}_2} = 0.086$, 0.090 nucleated at $x_{\text{CO}_2} \geq 0.092$ |
| CO ₂ solutions | 1 | TraPPE | TIP4P-Ice | 1.08* $\epsilon_{\text{O}(\text{CO}_2)\text{-O}(\text{H}_2\text{O})}$ | No. of CO ₂ 155-512 | nucleated at $x_{\text{CO}_2} \geq 0.088$ |

^aAll the systems contained 2944 water molecules. x_{CO_2} is pre-nucleation mole fraction of CO₂ in water; the number of CO₂ molecules is indicated for the CO₂ solution systems. ^bIn the CO₂ solution system containing 512 CO₂ (using the TraPPE model), CO₂ molecules quickly evolved in to a spherical CO₂ phase (Fig. S1H), thus this system was considered as a water/spherical CO₂ system.

All the simulations were performed at 250 K and 50 MPa using GROMACS v.5.0.6.⁶ Constant temperature and pressure were regulated by the Nosé-Hoover thermostat⁷ with a time constant of 2.0 ps and the Parrinello-Rahman barostat⁸ with a time constant of 4.0 ps, respectively. The periodic boundary conditions were imposed in three directions. A cutoff of 1.0 nm was used to estimate the short-range non-bonded interactions with the long-range corrections applied to energy and pressure. The electrostatic interactions were calculated with particle mesh Ewald method.⁹ The SETTLE algorithm¹⁰ was used to constrain the rigid geometry of water molecules. Trajectories were integrated using the leapfrog scheme with a time step of 2 fs and coordinates were stored every 10 ps.

As different CO₂ models and combining rules were tested to simulate CO₂ hydrate nucleation, the names of the CO₂ models are indicated in the figure captions. “**TIP4P-Ice_EPM2**” means the TIP4P-Ice water model, the EPM2 CO₂ model and the Lorentz-Berthelot combining rules for CO₂-water interaction were used. “**TIP4P-Ice_TraPPE**” means the TIP4P-Ice water model, the TraPPE CO₂ model and the Lorentz-Berthelot combining rules for CO₂-water interaction were used. “**TIP4P-Ice_1.08*TraPPE**” means the TIP4P-Ice water model, the TraPPE CO₂ model and *the well depth between the oxygen in CO₂ and the oxygen in water $\epsilon_{\text{O}(\text{CO}_2)\text{-O}(\text{H}_2\text{O})}$ scaled by a factor of 1.08* for CO₂-water interaction were used.

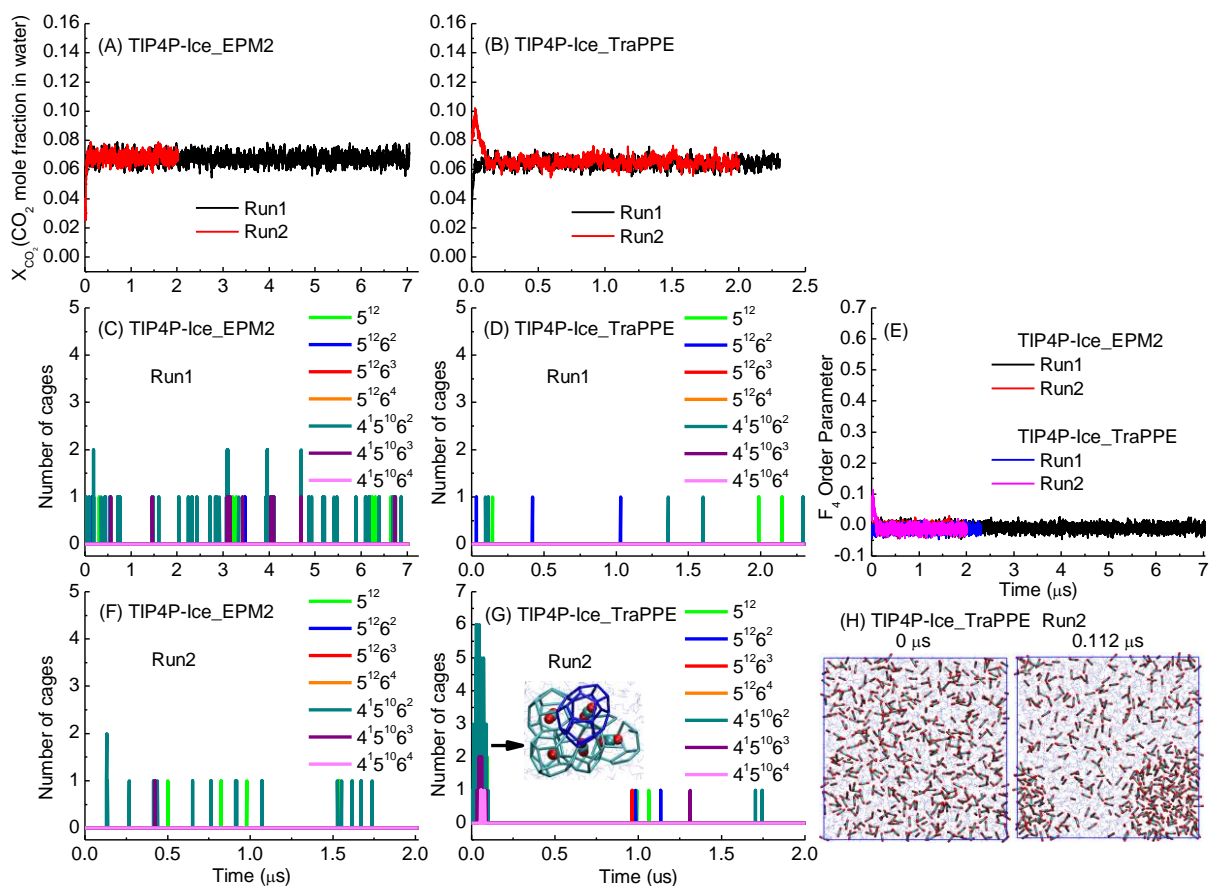


Fig. S1 Evolution of CO_2 mole fraction in water x_{CO_2} , F_4 order parameter (E), and cage number during the simulations using the Lorentz-Berthelot combining rules, TIP4P-Ice water model, EPM2 CO_2 model (A,C,F) or TraPPE CO_2 model (B,D,G) at 250 K and 50 MPa. All the starting configurations of these simulations contained water/ CO_2 two phases, except in Run2 using TraPPE model, a homogenous CO_2 solution was used as the starting configuration. Note that (H) in Run2 using TraPPE model, with CO_2 molecules aggregated to form CO_2 phase, the initial cage cluster dissociated (G) and x_{CO_2} decreased (B) to the equilibrated value as in Run1, i.e. Run2 is essentially the same as Run1 in later simulation duration.

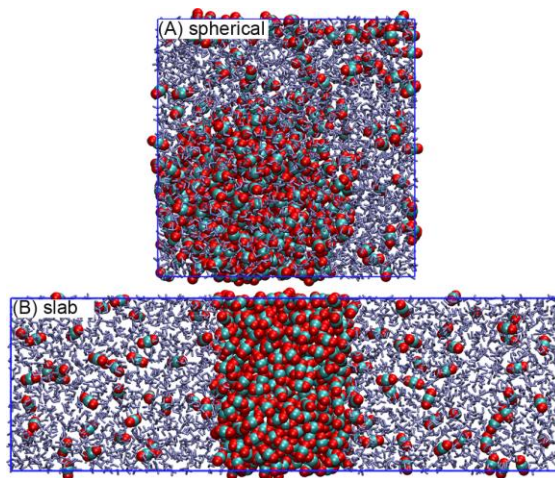


Fig. S2 Starting configurations containing a (A) spherical and (B) slab CO_2 liquid phase. Water molecules are shown as light blue sticks and CO_2 molecules are displayed as red and cyan balls.

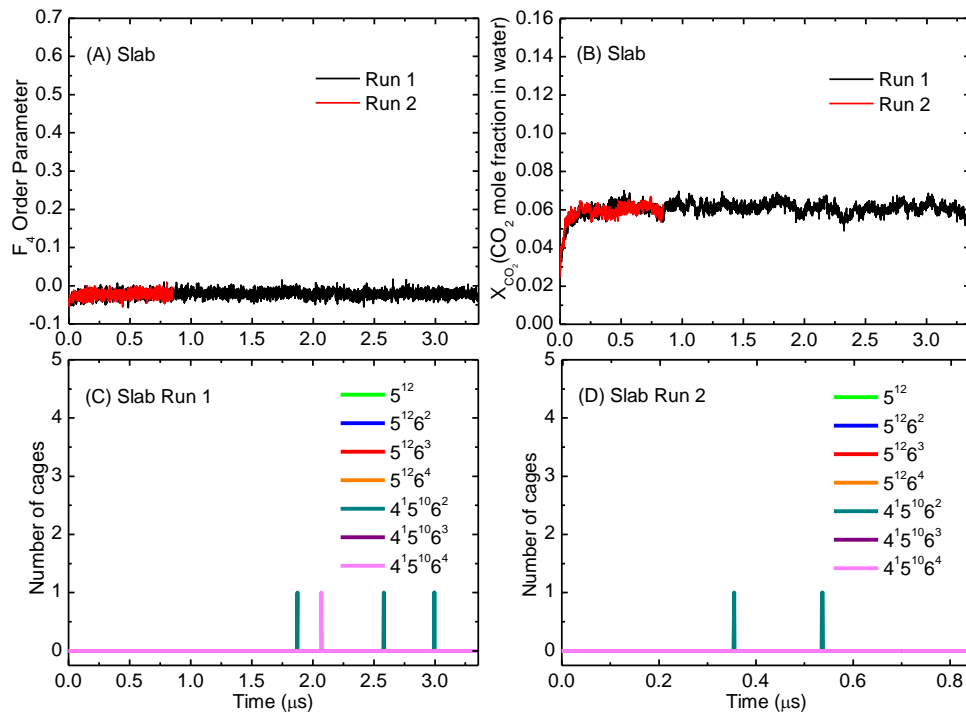


Fig. S3 (use **TIP4P-Ice_1.08*TraPPE**) Entire evolution of (A) F_4 order parameter, (B) CO_2 mole fraction in water x_{CO_2} and (C and D) number of cages for the system with slab CO_2 liquid phase.

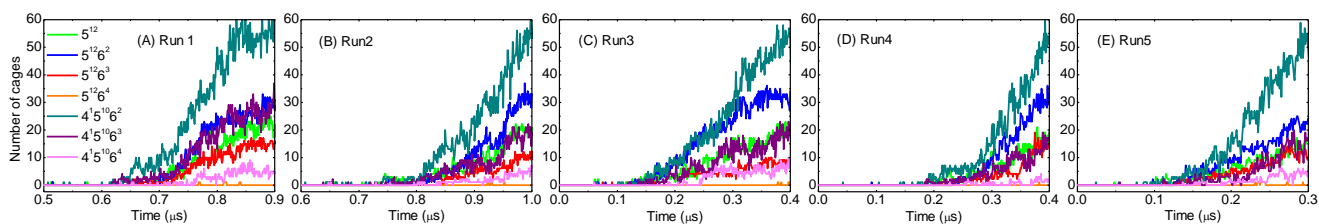


Fig. S4 (use **TIP4P-Ice_1.08*TraPPE**) Evolution of cage numbers during the nucleation and initial growth in the five repeated runs for the system with spherical CO_2 liquid phase.

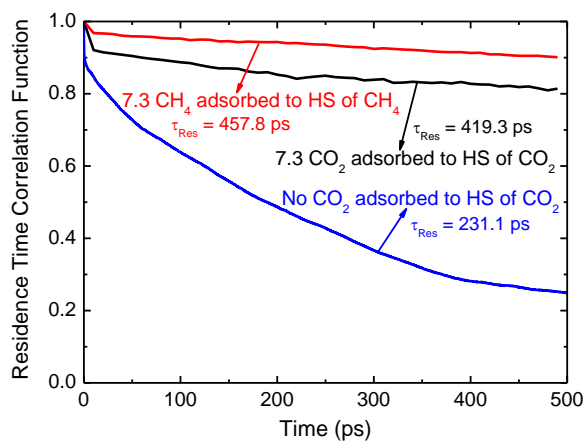


Fig. S5 (use **TIP4P-Ice_1.08*TraPPE**) Residence time correlation functions of water molecules in the hydration shells (HS) of CO_2 and CH_4 with different number of gas molecules adsorbed. The corresponding residence times τ_{Res} are indicated in the figure.

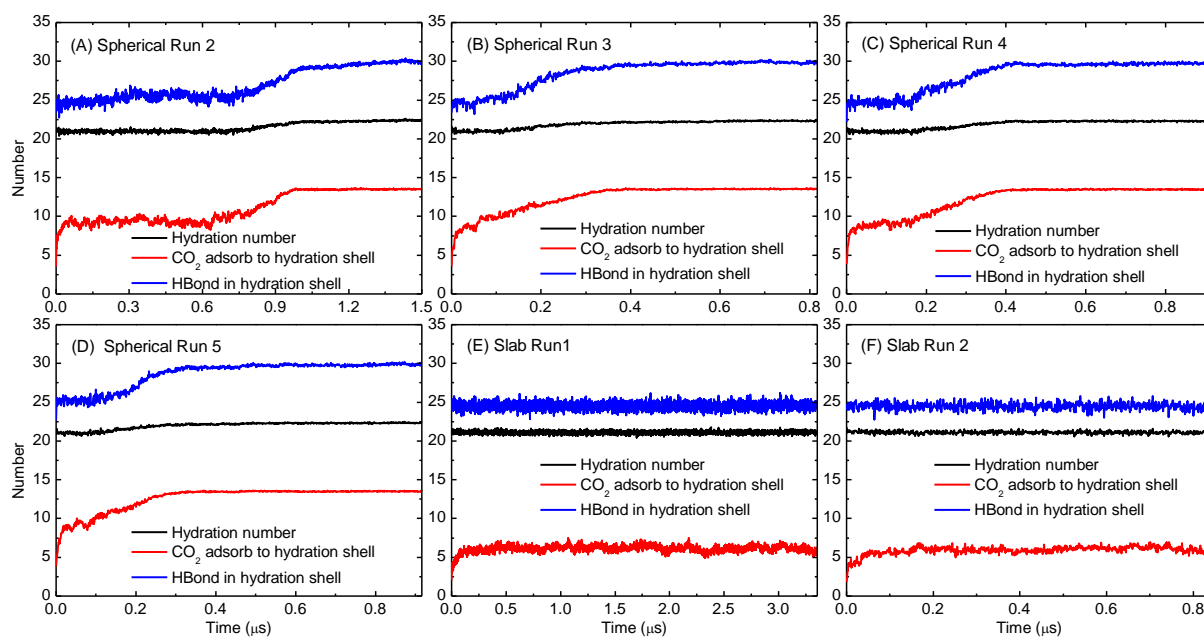


Fig. S6 (use **TIP4P-Ice_1.08*TraPPE**) Evolution of number of hydrogen bonds in CO₂ hydration shells, hydration number and number of CO₂ adsorbed to CO₂ hydration shells during the five repeated runs for the systems containing a spherical (A-D) and slab (E and F) CO₂ liquid phase. These numbers are averaged over all the dissolved CO₂ molecules.

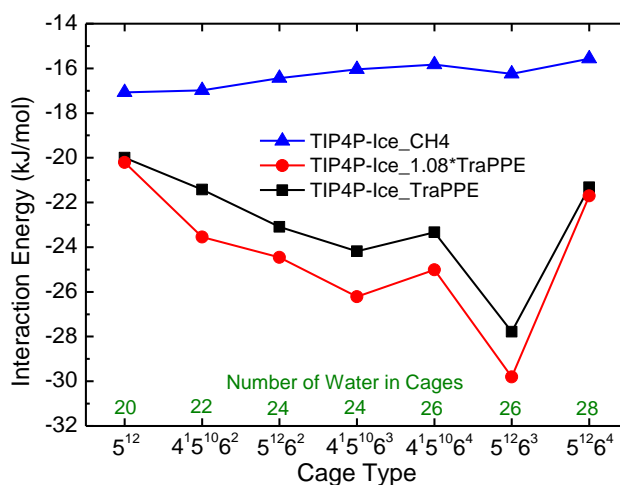


Fig. S7 Interaction energy between a CH₄ or CO₂ molecule and water molecules in the seven types of cages.

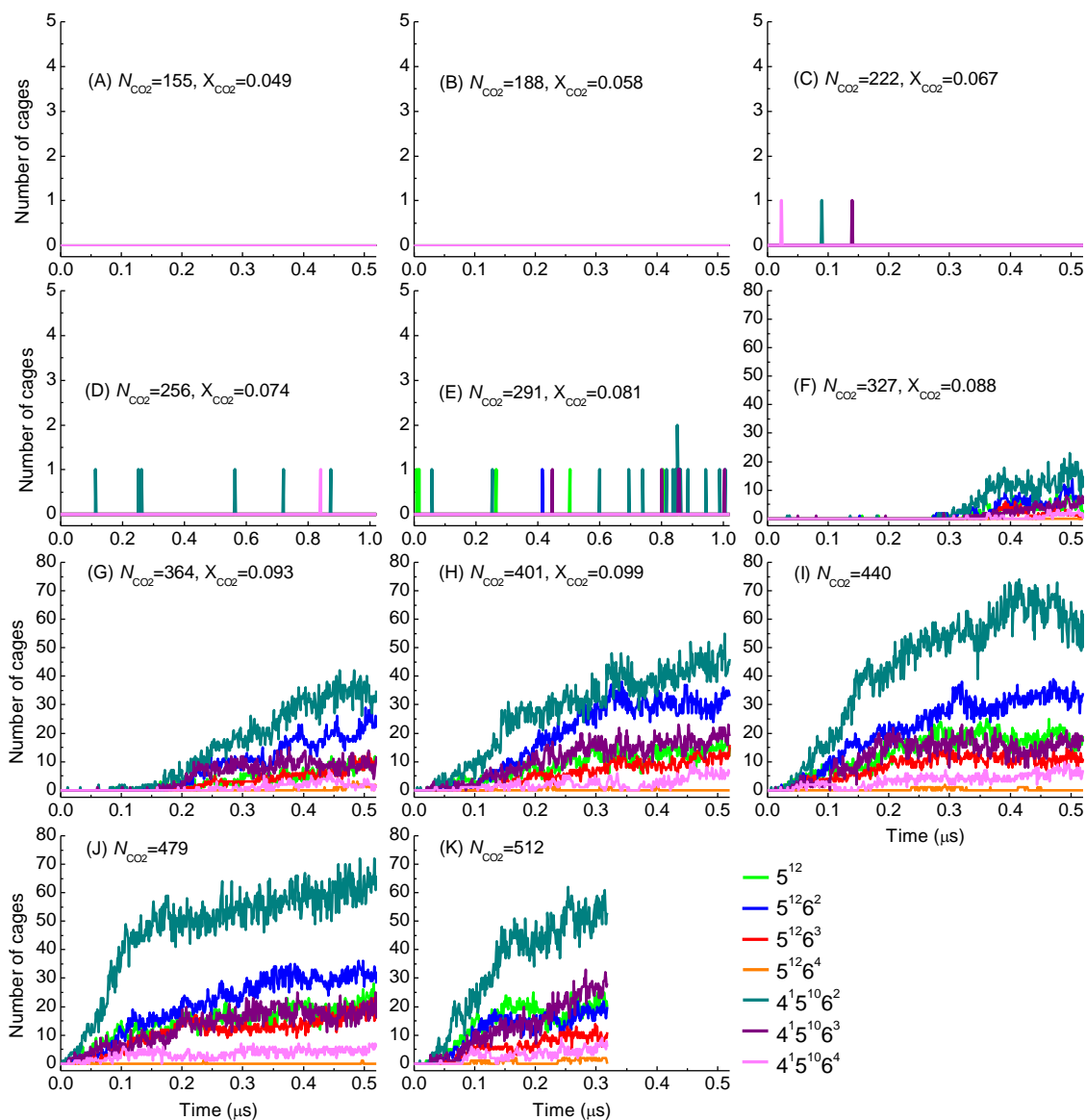


Fig. S8 (use **TIP4P-Ice_1.08*TraPPE**) Evolution of cage numbers during the simulations for CO₂ solution systems with different number of CO₂ (N_{CO_2}) and pre-nucleation x_{CO_2} .

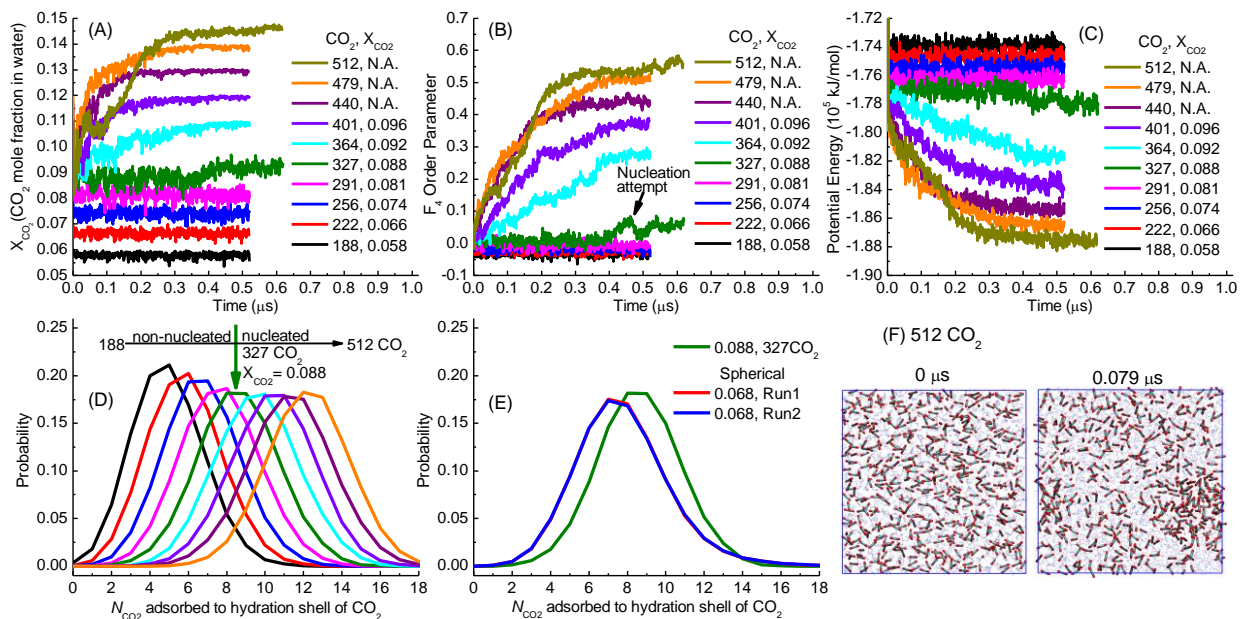


Fig. S9 (use TIP4P-Ice_EPM2) High aqueous guest concentration required for the nucleation of CO₂ hydrate. Evolution of (A) CO₂ mole fraction in water x_{CO_2} (B) F_4 order parameter, (C) potential energy and (D) distribution of number of CO₂ adsorbed to CO₂ hydration shells (N_{CO_2}) for CO₂ solution systems. The number of CO₂ in the systems and pre-nucleation x_{CO_2} are indicated in the legends. Note that only above or equivalent to the critical x_{CO_2} (about 0.088), hydrate nucleation occurs. (E) Comparing the distributions of N_{CO_2} in the non-nucleated system containing water/liquid CO₂ phase with $x_{CO_2} = 0.068$ (Fig. S1A) with that in CO₂ solution system with critical x_{CO_2} (0.088). (F) With the highest supersaturation (512 CO₂), some CO₂ molecules aggregate to form CO₂ phase at 0.079-0.1 μ s. Hydrate nucleation attempt was observed in CO₂ solution system with critical x_{CO_2} (0.088).

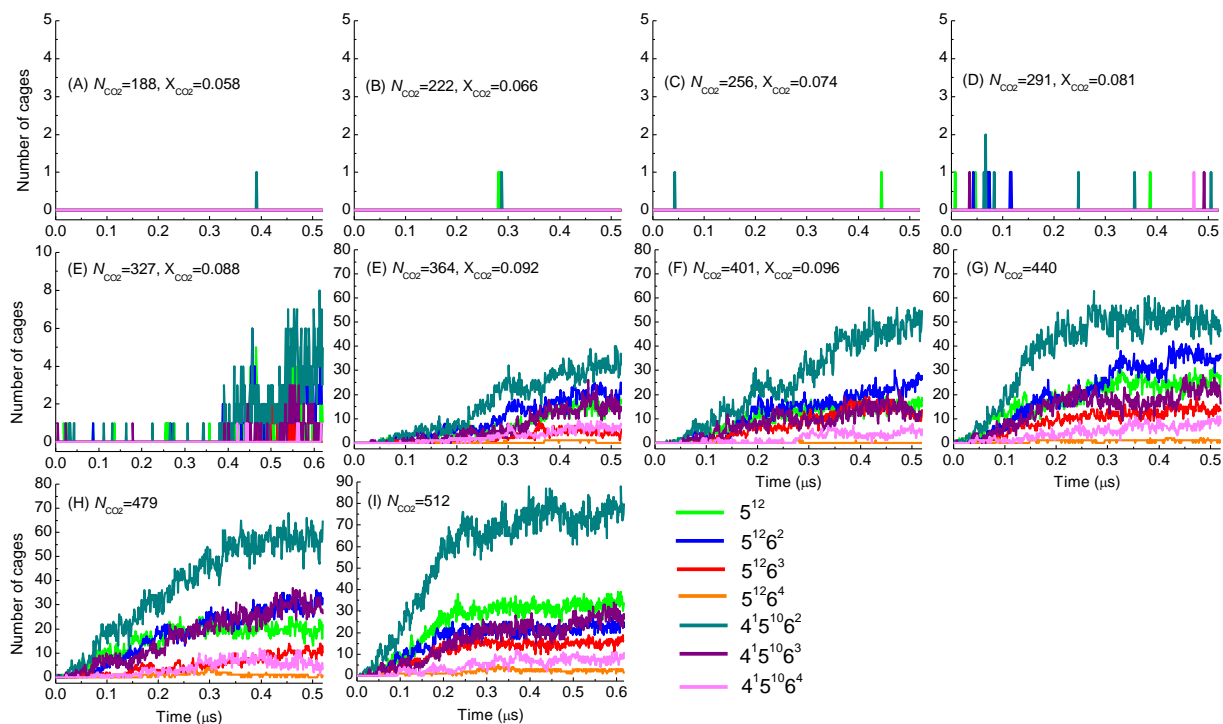


Fig. S10 (use TIP4P-Ice_EPM2) Evolution of cage numbers during the simulations for CO₂ solution systems with different number of CO₂ (N_{CO_2}) and pre-nucleation x_{CO_2} .

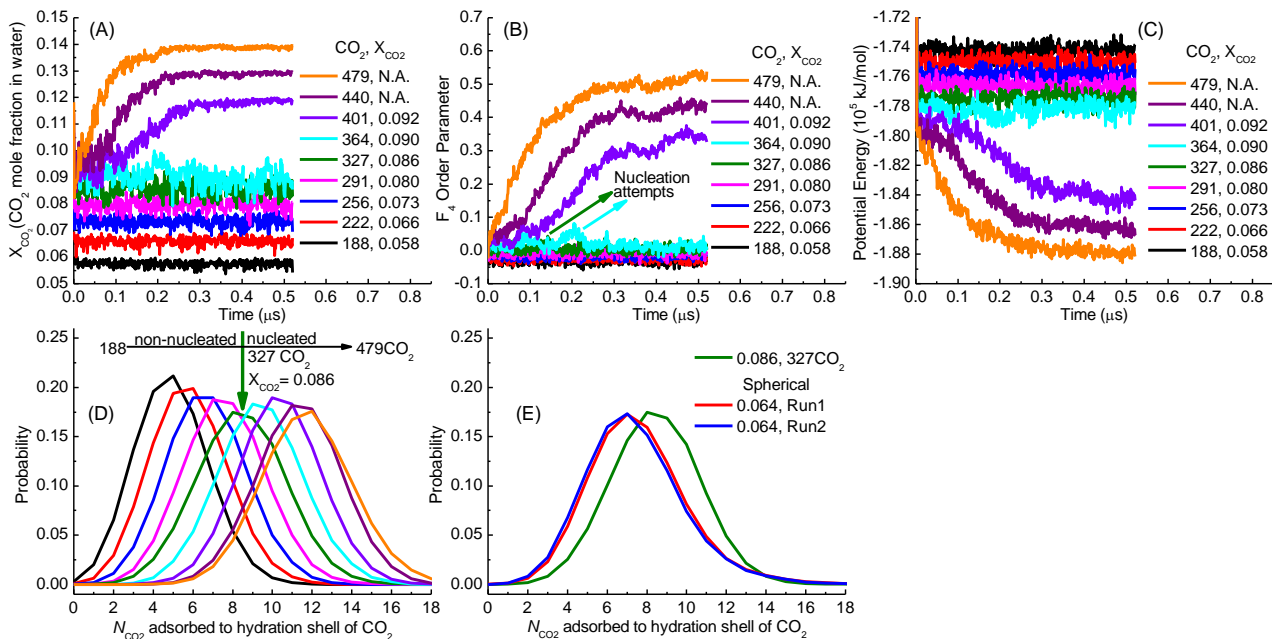


Fig. S11 (use TIP4P-Ice_TraPPE) High aqueous guest concentration required for the nucleation of CO₂ hydrate. Evolution of (A) CO₂ mole fraction in water x_{CO_2} (B) F_4 order parameter, (C) potential energy and (D) distribution of number of CO₂ adsorbed to CO₂ hydration shells (N_{CO_2}) for CO₂ solution systems. The number of CO₂ in the systems and pre-nucleation x_{CO_2} are indicated in the legends. *Note that only above or equivalent to the critical x_{CO_2} (about 0.092), hydrate nucleation occurs.* (E) Comparing the distributions of N_{CO_2} in the non-nucleated system containing water/liquid CO₂ phase with $x_{\text{CO}_2} = 0.064$ (Fig. S1B) with that in CO₂ solution system with $x_{\text{CO}_2} = 0.086$. *Note that in (B) hydrate nucleation attempts were observed in CO₂ solution systems with pre-nucleation $x_{\text{CO}_2} = 0.086$ and 0.090 .*

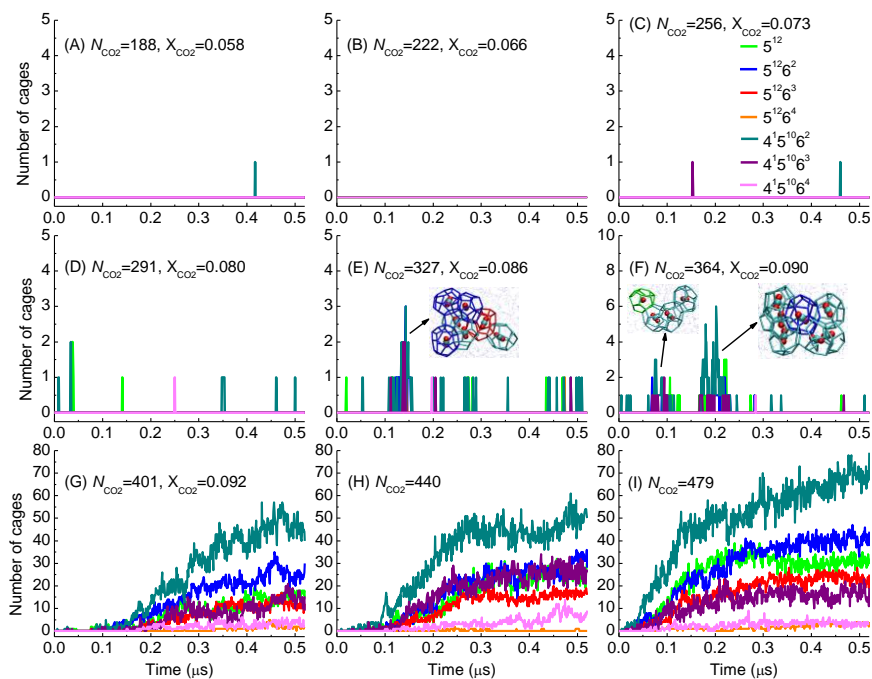


Fig. S12 (use TIP4P-Ice_TraPPE) Evolution of cage numbers during the simulations for CO₂ solution systems with different number of CO₂ (N_{CO_2}) and pre-nucleation x_{CO_2} . The insets in (E) and (F) show the cage clusters formed during hydrate nucleation attempts.

Video S1. Nucleation process of CO₂ hydrate. Water molecules and CO₂ (only carbon atom) are represented as light blue thin lines and red balls, respectively. Hydrate cages are shown as sticks with different colors (green for 5¹², blue for 5¹²6², red for 5¹²6³, orange for 5¹²6⁴, cyan for 4¹5¹⁰6², purple for 4¹5¹⁰6³ and pink for 4¹5¹⁰6⁴).

Video S2. Nucleation process of CH₄ hydrate. Water molecules and CH₄ are represented as light blue thin lines and green balls, respectively. One CH₄ molecule is highlighted as a violet large ball, around which other cages are formed and followed by hydrate growth. Hydrate cages are shown as sticks with different colors (green for 5¹², blue for 5¹²6², red for 5¹²6³, orange for 5¹²6⁴, cyan for 4¹5¹⁰6², purple for 4¹5¹⁰6³ and pink for 4¹5¹⁰6⁴). To compare the nucleation processes of CO₂ and CH₄ hydrates, Video S1 and Video S2 were generated with the same time interval.

References

- (1) He, Z. J.; Gupta, K. M.; Linga, P.; Jiang, J. W. Molecular Insights into the Nucleation and Growth of CH₄ and CO₂ Mixed Hydrates from Microsecond Simulations. *J. Phys. Chem. C* **2016**, *120*, 25225-25236.
- (2) Abascal, J. L. F.; Sanz, E.; Fernandez, R. G.; Vega, C. A Potential Model for the Study of Ices and Amorphous Water: TIP4P/Ice. *J. Chem. Phys.* **2005**, *122*, 234511.
- (3) Harris, J. G.; Yung, K. H. Carbon Dioxides Liquid-Vapor Coexistence Curve and Critical Properties as Predicted by a Simple Molecular-Model. *J. Phys. Chem.* **1995**, *99*, 12021-12024.
- (4) Potoff, J. J.; Siepmann, J. I. Vapor-Liquid Equilibria of Mixtures Containing Alkanes, Carbon Dioxide, and Nitrogen. *AIChE J.* **2001**, *47*, 1676-1682.
- (5) Costandy, J.; Michalis, V. K.; Tsimpanogiannis, I. N.; Stubos, A. K.; Economou, I. G. The Role of Intermolecular Interactions in the Prediction of the Phase Equilibria of Carbon Dioxide Hydrates. *J. Chem. Phys.* **2015**, *143*, 094506.
- (6) Hess, B.; Kutzner, C.; van der Spoel, D.; Lindahl, E. Gromacs: Algorithms for Highly Efficient, Load-Balanced, and Scalable Molecular Simulation. *J. Chem. Theory Comput.* **2008**, *4*, 435-447.
- (7) Nose, S. A Molecular Dynamics Method for Simulations in the Canonical Ensemble. *Mol. Phys.* **1984**, *52*, 255-268.
- (8) Parrinello, M.; Rahman, A. Crystal Structure and Pair Potentials: A Molecular-Dynamics Study. *Phys. Rev. Lett.* **1980**, *45*, 1196-1199.
- (9) Darden, T.; York, D.; Pedersen, L. Particle Mesh Ewald: An N.Log(N) Method for Ewald Sums in Large Systems. *J. Chem. Phys.* **1993**, *98*, 10089-10092.
- (10) Miyamoto, S.; Kollman, P. A. Settle: An Analytical Version of the Shake and Rattle Algorithm for Rigid Water Models. *J. Comput. Chem.* **1992**, *13*, 952-962.